



Monocline development by oblique-slip fault-propagation folding: the East Kaibab monocline, Colorado Plateau, Utah

Sarah E. Tindall*, G.H. Davis

Department of Geosciences, The University of Arizona, Tucson, AZ 85721, USA

Received 18 May 1998; accepted 28 March 1999

Abstract

Fault relationships along a 50-km stretch of the East Kaibab monocline in southern Utah suggest that Late Cretaceous/early Tertiary development of the structure involved a significant component of right-lateral strike-slip displacement, accommodated by basement-rooted faulting and fault-propagation folding. Evidence of oblique slip is provided mainly by pervasive map-scale and outcrop-scale faults that define a shear zone occupying the steep east-dipping limb of the monocline for at least its northernmost 50 km. Dominant fault orientations are synthetic and antithetic to the shear zone, and accommodate reverse-right-lateral and reverse-left-lateral slip, respectively. Structural style within the shear zone changes character and increases in intensity with progressively lower structural and stratigraphic levels in the fold, suggesting that the shear zone propagated upward from a basement-rooted fault during monocline formation. We conclude that horizontal, ENE-directed, Laramide compression drove reverse-right-lateral slip on the basement fault zone beneath the developing East Kaibab monocline. The resulting transpressional fault-propagation fold is marked in southern Utah by 1600 m of reverse displacement and possibly 8000 m of right-lateral displacement across the shear zone and associated monoclinical flexure. © 1999 Elsevier Science Ltd. All rights reserved.

1. Background

1.1. Monoclines as drape folds

The formation of regionally significant monoclines like those on the Colorado Plateau of the western United States has most often been explained as the result of drape folding of a sedimentary rock sequence above near-vertical, normal or reverse faults in underlying basement. Early explorers of the Colorado Plateau and Grand Canyon regions described monoclinical flexures, and recognized a relationship between folding in the Paleozoic and Mesozoic sedimentary sequence and faulting at depth (Powell, 1873; Dutton, 1882; Walcott, 1890). Most Colorado Plateau monoclines exposed in the Grand Canyon (e.g. East Kaibab, West Kaibab, Hurricane, Grandview) lie above steeply

dipping basement faults; these faults formed during Precambrian time, and underwent reverse reactivation during Late Cretaceous/early Tertiary (Laramide) deformation (Walcott, 1890; Maxson, 1961; Huntoon, 1969, 1971, 1974; Huntoon and Sears, 1975; Reches, 1978).

Many authors have proposed that Colorado Plateau monoclines formed by drape folding, defined as the passive response of a sedimentary cover sequence to faulting in the basement beneath (Sanford, 1959; Prucha et al., 1965). Stearns (1971) discussed the development of drape folds in the Rocky Mountain foreland province, and extended his observations to the Colorado Plateau monoclines. In his descriptions, drape folds occur where faulting is the primary deformation mechanism in the basement, but folding dominates in the sedimentary cover, i.e. faulting in the sedimentary cover is of minor importance (Stearns, 1971). The transition from fault to fold is accomplished by detachments and thinning in the above-basement sedimentary sequence, particularly aided by

* Corresponding author. Fax: +1-520-621-2672.
E-mail address: set@u.arizona.edu (S.E. Tindall)

extreme thinning of weak sedimentary rocks immediately overlying the basement (Stearns, 1971). Reches and Johnson (1978) determined that the Palisades Creek branch of the East Kaibab monocline in the Grand Canyon region resulted from a combination of buckling and drape folding above a near-vertical fault. According to Reches (1978), the mechanism of deformation of the drape-folded cover is virtually independent of the type of basement deformation (e.g. faulting, igneous intrusion, or local steepening of layers).

1.2. *Monoclines as fault-propagation folds*

According to Suppe (1985), a fault-propagation fold represents deformation immediately in front of a propagating fault tip. By this broad definition, drape folds might be considered as a subset of fault-propagation folds. However, implicit in fault-propagation fold models is the idea that fault-accommodated offset progressively gives way to fold-accommodated offset with higher structural and stratigraphic levels, and that with continued deformation the fault will propagate through the fold (Suppe and Medwedeff, 1984; Jamison, 1987). In drape folding, fault offset simply dies out just above basement in the sedimentary cover.

Although fault-propagation fold models were originally developed to analyze 'thin-skinned' fold-thrust belt geometry (Suppe and Medwedeff, 1984), the term fault-propagation fold has been extended to include folding associated with basement-cored uplifts like those of the Rocky Mountain foreland of the western United States (e.g. Erslev, 1991; Erslev and Rogers, 1993; Stone, 1993; Mitra and Mount, 1998). Stone (1984, 1993) proposed that use of the term fault-propagation fold be reserved for application to areas of thin-skinned fold-thrust belt structures, and that the term thrust-fold be adopted for basement-involved deformation like that seen in the Rocky Mountain foreland. Admittedly the two structural styles differ, but the term 'thrust-fold' implies dip-slip kinematics, a connotation that might result in confusion if applied to areas of wrench faulting or oblique deformation. The broad definition of fault-propagation fold captures the simultaneous development of fault and fold for both thin-skinned and basement-cored structures without specifying slip direction. Following Erslev (1991), Erslev and Rogers (1993) and Mitra and Mount (1998), the term fault-propagation fold is used here to describe folding associated with basement-involved deformation in the study area.

Colorado Plateau monoclines have not been excluded from basement-cored fault-propagation fold models, but they have not been cited as prime examples of fault-propagation folding. One reason may be that offset across Colorado Plateau structures

is small compared to structural relief in the Rocky Mountain foreland, so that fault-propagation fold characteristics (if present) are less developed. In addition, in Grand Canyon exposures of the monoclines, basement-rooted faulting gives way to unfaulted folding very low in the Paleozoic (above-basement) section (Huntoon, 1971, 1993; Reches, 1978; Reches and Johnson, 1978; Huntoon et al., 1996), a characteristic that seems to support the drape fold model.

It is important to note, however, that Grand Canyon exposures do not necessarily coincide with locations of greatest structural relief, or greatest offset, on the monoclines and their associated faults. For example, the East Kaibab monocline exhibits 1600 m of structural relief in southern Utah, but only 800 m of vertical relief in the Grand Canyon (Babenroth and Strahler, 1945). In a fault-propagation fold, basement-rooted faulting should extend higher into the sedimentary cover in areas of greater structural relief than in areas of lesser offset. Map relationships in southern Utah, where the East Kaibab monocline has its greatest structural relief, demonstrate that the structure developed through fault-propagation folding, not drape folding.

1.3. *Importance of oblique deformation*

Drape-fold and fault-propagation fold models are usually presented in vertical cross-section. This view indirectly encourages the assumption that principal stress and strain directions are exactly parallel and perpendicular to the plane of the cross-section. For the sake of simplicity, oblique movement of material relative to the cross-section plane is seldom considered. Such simplified constructions may produce reasonable interpretations when applied to individual structures, but can lead to confusion in interpretation of regional kinematics.

For example, basement-cored uplifts tend to occupy a wide range of orientations, with no clear regional sense of vergence (e.g. Colorado Plateau monoclines, Rocky Mountain foreland uplifts and Ancestral Rockies). No single compression direction seems capable of producing reverse reactivation of structures with such variable trends. Stearns (1978) promoted the idea that vertical uplift, perhaps caused by a vertically oriented greatest principal stress (σ_1), accounted for the variable orientations and steeply dipping basement faults associated with Colorado Plateau and Rocky Mountain uplifts. Since then, several authors have shown that the Laramide stress which drove basement reactivation and monoclinical folding on the Colorado Plateau was horizontal and compressive, not vertical (Reches, 1978; Huntoon, 1981; Anderson and Barnhard, 1986). Given a horizontal compressive stress, Chapin and Cather (1983) hypothesized two

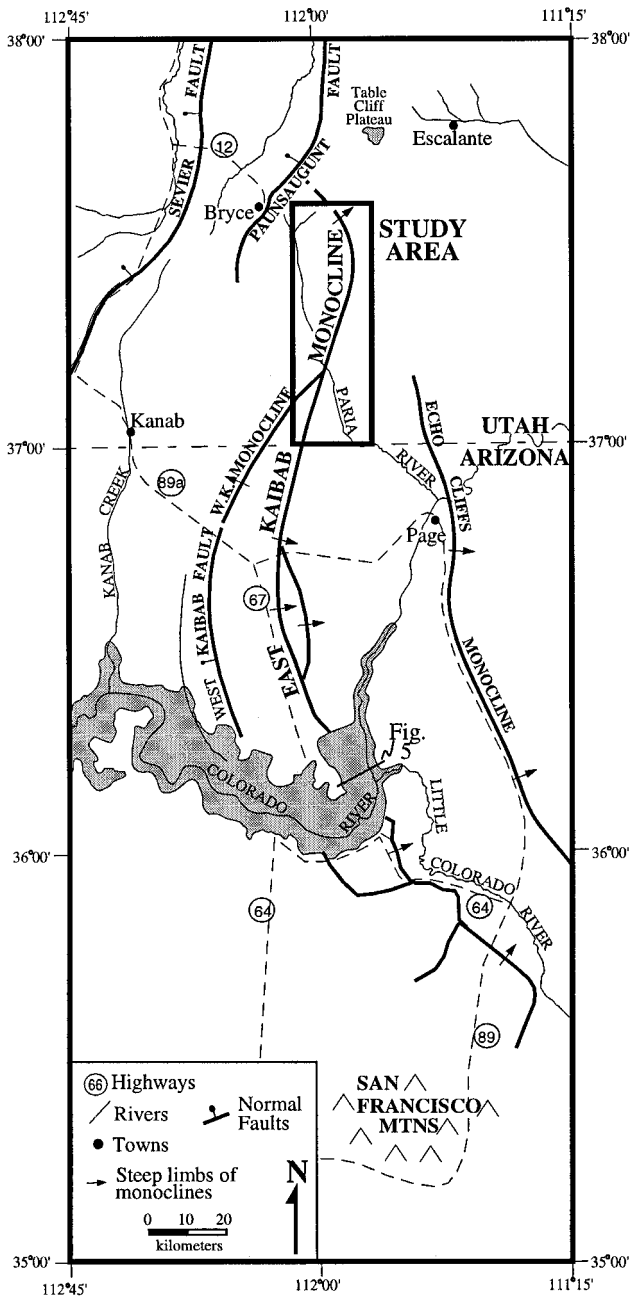


Fig. 1. Location and geologic setting of the East Kaibab monocline. The southern Utah study area is outlined, and the location of Fig. 5 (in the Grand Canyon) is shown.

stages of Laramide deformation, marked by a change in the compression direction, to explain the disparate trends of the uplifts.

Despite the apparent difficulty in reactivating a steeply dipping fault with a horizontal compressive stress, most studies of Colorado Plateau uplifts imply that Laramide compression produced reverse, dip-slip motion on the basement faults (e.g. Huntoon, 1971, 1981, 1993; Davis, 1978; Reches, 1978; Stearns, 1978). Among the exceptions are studies by Stone (1969) and

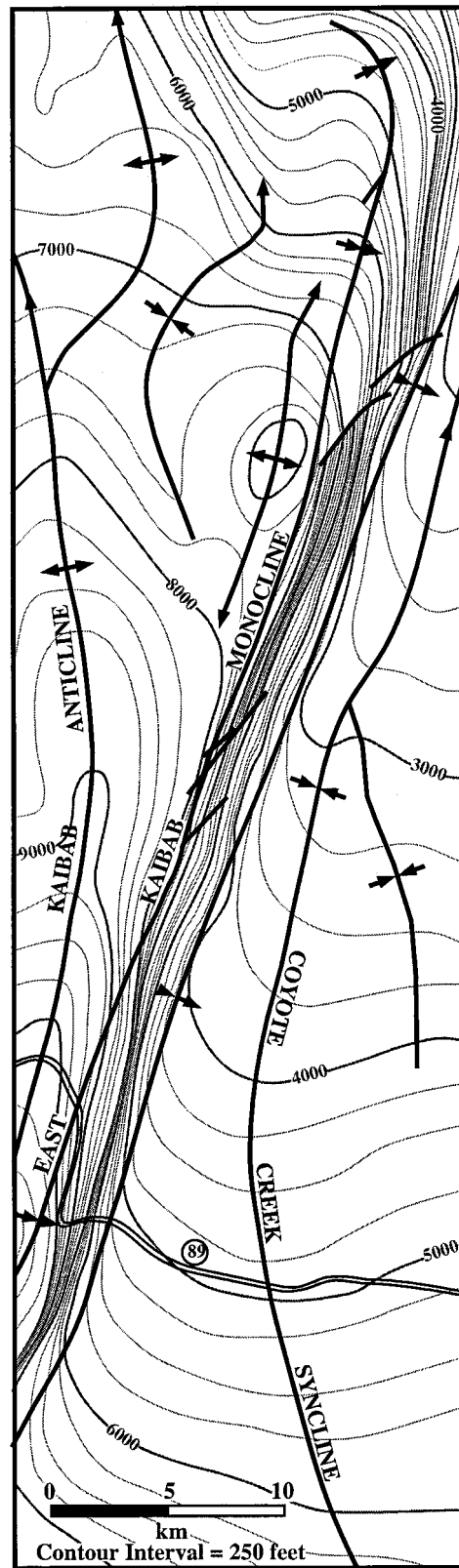


Fig. 2. Structure contour map of the northern East Kaibab monocline. Structure contours, in feet, drawn on the base of the Cretaceous Dakota Sandstone. Modified from Gregory and Moore (1931).

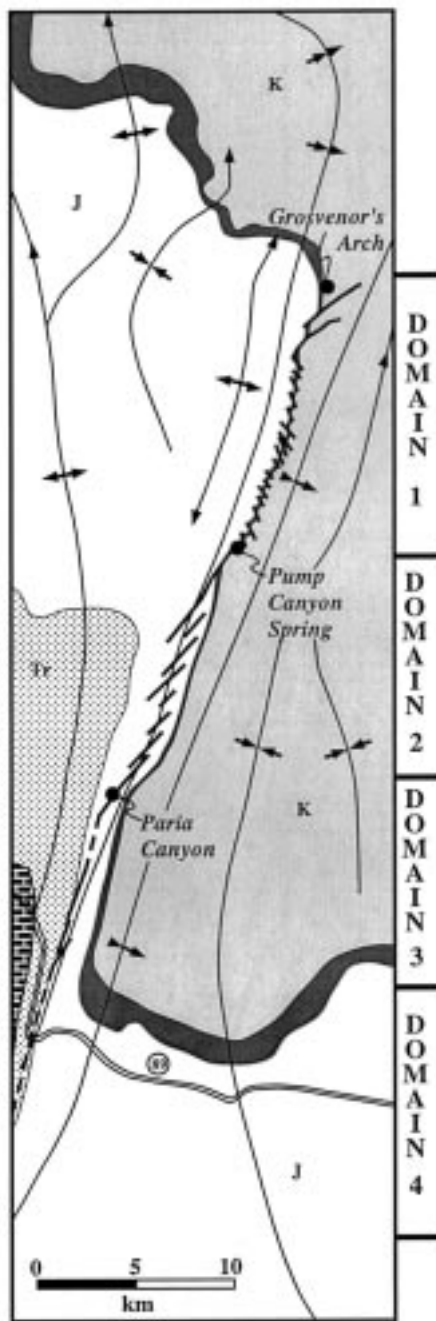


Fig. 3. Simplified geologic map of the study area. Permian, Triassic, Jurassic, and Cretaceous rocks are shaded differently to emphasize the slight northward plunge of the monocline. Note that faulting and folding in the steep limb move from older stratigraphic units in the south into higher stratigraphic units northward. The relatively thin Cretaceous Dakota Sandstone is shaded black to highlight left-lateral separations on faults at the north end of the monocline. Geographical features and structural domains discussed in the text are labeled.

Davis (1978) which pointed out that pre-existing basement fractures of many orientations could be reactivated by a horizontal compressive stress. This would

| | | FORMATION | TH (m) | LITHOLOGY |
|---------------|--------------------------------------|-------------------------------------|----------|-----------|
| Q | | Surficial deposits | 0-200 | Qal |
| TERT | | Claron Formation | 350-600 | TKc |
| | | fresh-water limestone | | |
| CRETACEOUS | | Kaiparowits Fm. | 350-1000 | Kk |
| | | interbedded sandstone and siltstone | | |
| | | Wahweap Formation | 300-500 | Kw |
| | | interbedded sandstone and siltstone | | |
| | | StraightCliffs Formation | 400-600 | Ksc |
| | interbedded sandstone and siltstone | | | |
| | Tropic Shale | 200-400 | Kt | |
| | coal-bearing shale | | | |
| | Dakota Formation | 30-100 | Kd | |
| | sandstone, conglomerate | | | |
| JURASSIC | | Entrada Sandstone | 150-270 | Je |
| | | poorly-consolidated sand and silt | | |
| | | Carmel Formation | 150-300 | Jc |
| | | shale, gypsum, limestone | | |
| | Page Ss Member | 5-50 | Jcp | |
| | aeolian sandstone (Carmel Fm member) | | | |
| | Navajo Sandstone | 350-650 | Jn | |
| | aeolian sandstone | | | |
| TRIASSIC | | Kayenta Formation | 40-150 | Jk |
| | | sandstone, siltstone | | |
| | | Moenave Formation | 25-150 | Trmv |
| | sandstone, siltstone | | | |
| | Chinle Formation | 175-250 | Trc | |
| | shale, sandstone, conglomerate | | | |
| | Moenkopi Formation | 350-550 | Trmo | |
| | shale, siltstone, limestone, gypsum | | | |
| PERMIAN | | Kaibab Limestone | 40-100 | Pk |
| | | limestone, dolomite | | |
| | | Toroweap Formation | 40-150 | Pt |
| | | anhydrite | | |
| | Coconino Sandstone | 80-150 | Pc | |
| | sandstone | | | |
| | Hermit Shale | 100 | Ph | |
| | shale | | | |
| MISSISSIPPIAN | | Supai Group | 180-400 | PPps |
| | | shale, siltstone, sandstone | | |
| MISSISSIPPIAN | | Surprise Canyon Fm | 0-130 | Msc |
| | | siltstone, sandstone | | |
| MISSISSIPPIAN | | Redwall Limestone | 100-250 | Mr |
| | | cherty limestone | | |
| DEVONIAN | | Temple Butte Ls | 0-100 | Dtb |
| | limestone | | | |
| CAMBRIAN | | Muav Limestone | 100-300 | €m |
| | | limestone | | |
| | | Bright Angel Shale | 75-200 | €ba |
| | shale | | | |
| CAMBRIAN | | Tapeats Sandstone | 0-100 | €t |
| | | sandstone | | |
| PRE-CAMBRIAN | | Grand Canyon Series | 275+ | p€ |
| | Proterozoic sediments | | | |

Fig. 4. Generalized stratigraphic column for the East Kaibab monocline in southern Utah. Shaded units are used as markers to highlight structural relationships on maps of Domains 1 through 4. Stratigraphy compiled from Hintze (1988).

account for the wide range in structural trends, and would also result in oblique deformation on some structures. The possibility of basement-rooted oblique motion across Colorado Plateau monoclines has been suggested in studies by Barnes (1974, 1987), Ohlman (1982) and Karlstrom and Daniel (1993), but detailed field documentation is lacking. Fault relationships discussed here not only suggest suggest basement-rooted fault-propagation folding, but also indicate that a significant component of right-lateral slip took place during Laramide formation of the East Kaibab monocline in southern Utah. This in turn opens up new possibilities for interpreting the Colorado Plateau monoclines as a system.

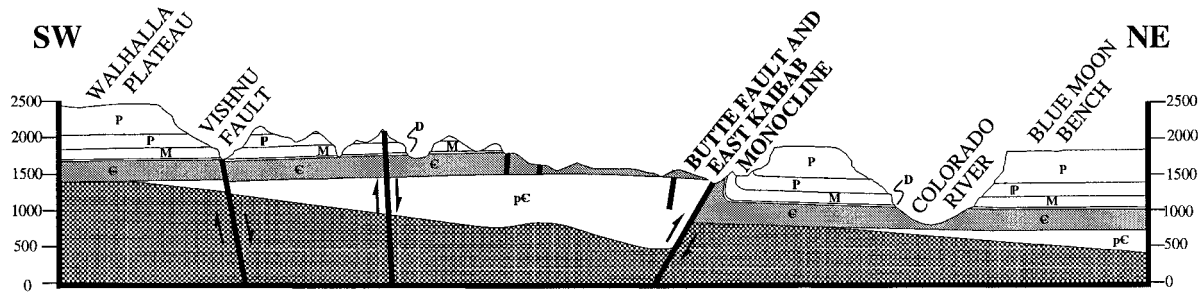


Fig. 5. The East Kaibab monocline and underlying Butte fault in the Grand Canyon. Lower Proterozoic and Cambrian rocks are shaded to emphasize the apparent normal offset at the level of Precambrian sedimentary rocks, and reverse separation at the Proterozoic–Phanerozoic unconformity. Location of the cross-section is shown in Fig. 1. After Huntoon et al. (1996).

2. Geological setting

The Kaibab Uplift of northern Arizona and southern Utah is a north–south trending, asymmetrical anticline near the western margin of the Colorado Plateau. The moderately to steeply dipping east limb of the uplift, the East Kaibab monocline, meanders for approximately 180 km from near Bryce, Utah to just north of Flagstaff, Arizona (Fig. 1). The 50-km long Utah segment of the monocline, which is the subject of this paper, shows structural relief of 1600 m between the anticlinal crest of the uplift and the synclinal trough of the monocline, based on structural contouring of the base of the Dakota Sandstone (Gregory and Moore, 1931; Fig. 2). The East Kaibab monocline trends N20°E from the Arizona–Utah border to Bryce, where the monocline and the Kaibab Uplift die out; both structures plunge approximately 5° northward.

The slight northward plunge of the Utah segment of the East Kaibab monocline creates an insightful perspective of the structure in map view (Fig. 3). The steep limb of the fold occupies progressively older strata when followed from north to south. Cretaceous units form the steep limb in the north near Grosvenor's Arch, Jurassic rocks are intensely deformed at Paria Canyon, and Triassic and Permian rocks define the steep limb where Highway 89 crosses the fold. Although up to 2000 m of folded and faulted Proterozoic and Paleozoic sedimentary rocks lie between crystalline basement and the Kaibab Limestone, these are not exposed in the study area (Fig. 4).

The timing of monocline formation is poorly constrained. At the north end of the structure, Cretaceous Wahweap and Kaiparowits Formations have been eroded from the crest of the uplift but are exposed on its flanks, where dips range from 40° near Grosvenor's Arch to 0° in the vicinity of Table Cliff Plateau. These Late Cretaceous rocks were clearly deposited before folding. Paleocene rocks between Grosvenor's Arch and Table Cliff are synclinally folded, probably as a result of Laramide deformation as well (Sargent and

Hansen, 1982). Eocene strata lie unconformably on the Late Cretaceous units at Table Cliff (Gregory and Moore, 1931; Bowers, 1972) but have been stripped from the folded edges of the Kaibab Uplift (Sargent and Hansen, 1982). The Eocene rocks may or may not have been affected by folding; their presence does not provide an upper time limit for monocline formation.

Deep exposures in the Grand Canyon reveal that a steeply west-dipping (70°) basement fault zone underlies the East Kaibab monocline. Grand Canyon outcrops provide clear evidence that the basement structure originally formed as a normal fault in Precambrian times (Walcott, 1890; Maxson, 1961; Huntoon, 1969, 1993; Huntoon and Sears, 1975) but that the only Phanerozoic deformation on the fault resulted from Laramide compression (Fig. 5). This episode produced reverse separation across the fault at the level of the Proterozoic/Phanerozoic unconformity in the Grand Canyon and formed the broad, asymmetrical Kaibab Uplift in the Paleozoic and Mesozoic cover (Huntoon and Sears, 1975; Huntoon, 1993). Although the Grand Canyon provides the only exposure of the basement fault underlying the East Kaibab monocline, the fault (or a network of similar faults) is assumed to underlie the fold for its entire length (Davis, 1978; Stern, 1992).

3. Structural data and observations

Examination of the northern 50 km of the East Kaibab monocline has revealed a continuous, N20°E-trending, monocline-parallel zone of intense deformation expressed at map scale by abundant, systematic faulting within the steep limb. Map-scale and outcrop-scale structures in the deformed zone indicate a significant component of reverse-right-lateral offset. When followed south from Grosvenor's Arch to the Arizona–Utah border, this narrow zone of faulting 'steps' progressively southwestward and stratigraphically downward through Cretaceous, Jurassic, and Triassic strata. Structural style within the zone changes

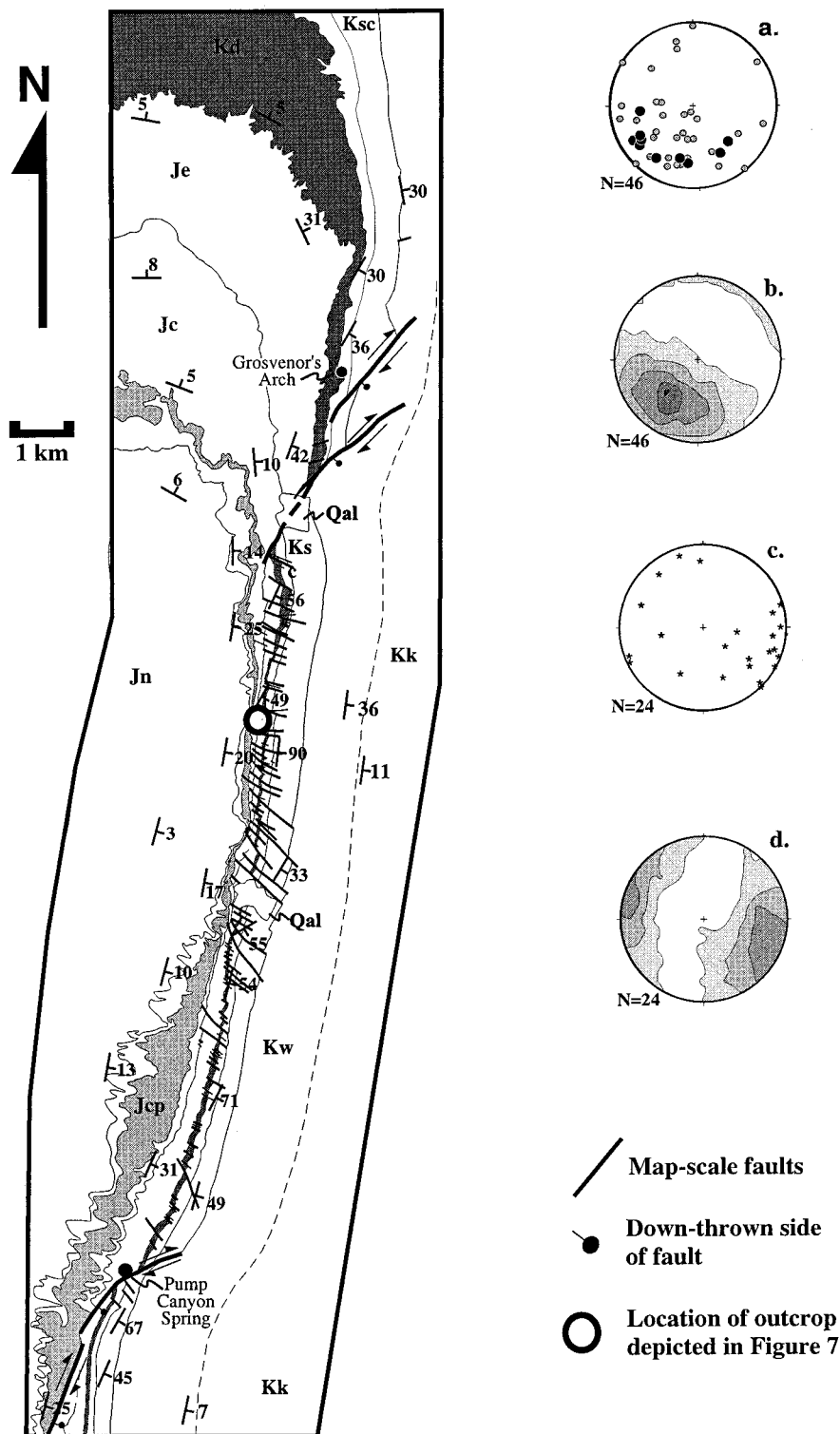


Fig. 6. Geology of Structural Domain I. Short, northwest-striking, northeast-dipping faults offset Cretaceous Dakota Sandstone (dark shading) in an apparent left-lateral fashion. At the northern and southern boundaries, northeast-striking, northwest-dipping faults accommodate reverse, right-lateral offset. East of (and stratigraphically above) the northeast-striking faults at north and south ends, the right-lateral offset results in broad, z-shaped bends in the contact between Cretaceous Wahweap and Kaiparowits Formations. Equal-area plots summarize structural data: (a) Plot of poles to planes. Poles to faults are shown in black; poles to outcrop-scale slip surfaces are shown in grey. (b) Kamb contour plot of poles to faults and slip surfaces. Shades represent 2σ contour intervals. White areas indicate fewer poles at contouring grid points than would be found in a uniform distribution minus 1σ ; light grey shading indicates grid points with number of poles within $\pm 1\sigma$ of that found in a uniform distribution; slightly darker grey shading indicates grid points with numbers of poles $1-3\sigma$ more than in a uniform distribution, etc. (c) Slickenline orientations. (d) Kamb contour plot of slickenlines, emphasizing their low plunge and southeast trend.



Fig. 7. Southwest-directed photograph of the graded road surface in Domain 1 (outcrop location is circled on Fig. 6). Northwest-striking faults offset northeast-striking, east-dipping shales and evaporites of the Carmel Formation. Geologist is Pilar Garcia.

from north to south as well, allowing subdivision of the Utah portion of the East Kaibab monocline into four domains based on style of deformation and stratigraphic interval (Fig. 3). The fault pattern in each domain and in the transitions between domains provides evidence for oblique slip fault-propagation folding, as discussed in the following sections.

3.1. Domain 1

Structural Domain 1 begins near Grosvenor's Arch in Grand Staircase–Escalante National Monument, and extends about 15 km toward S20°W to Pump Canyon Spring (Fig. 6). A 10 km-long, monocline-parallel zone of short, closely spaced, northwest-striking faults occupies the stratigraphic interval of Jurassic Page Sandstone through Cretaceous Tropic Shale. Strata within the zone are offset by meters to tens of meters in apparent left-lateral fashion and are rotated clockwise by the northwest-striking faults.

More than 75 of these northwest-striking, northeast-dipping faults are visible in Domain 1 at 1:12 000 scale. Trace lengths of the largest faults are on the order of 0.5–1 km. The faulting is pervasive in outcrop

as well, with sub-map-scale faults evident on the graded surface of the dirt road, where they offset steeply east-dipping, thin-bedded shales and evaporites in the Carmel Formation (Fig. 7). Average strike and dip of map-scale and outcrop-scale faults are N50°W, 58°NE with slickenlines (found on fault surfaces preserved in the Dakota Formation and the Page Sandstone member of the Carmel Formation) that rake 20°SE. Fault and slickenline orientations suggest that at least the latest slip along these short faults was left-lateral with a small reverse component.

To the north, near Grosvenor's Arch, the monocline-parallel zone of northwest-striking faults ends abruptly at two northeast-striking faults, each with a trace length of about 3 km. These faults accommodate apparent right-lateral separation of the Jurassic Carmel through Cretaceous Wahweap Formations. Strike-parallel offset of the Cretaceous Dakota Sandstone is on the order of 1 km across each fault, but appears to decrease to the northeast (stratigraphically upward) into the Straight Cliffs and Wahweap Formations. Where preserved, the fault surfaces strike N65°E and dip 65°NW. Slickenlines rake 15–20°SW, disclosing at least a late-stage episode of reverse-right-lateral displacement. These northeast-striking faults occupy a higher stratigraphic interval than do the northwest-striking faults between Grosvenor's Arch and Pump Canyon Spring. Northeast of the faults themselves, in Cretaceous Wahweap and Kaiparowits Formations, lateral displacement is accommodated by a broad, z-shaped folding of the trend of the monocline, suggestive of right-handed shear (see contact between Kw and Kk, Fig. 6).

Faults at the southern termination of Domain 1 are similar to the northeast-striking faults at the northern end, but occupy a lower stratigraphic interval. Near Pump Canyon Spring, the zone of northwest-striking faults ends abruptly near a northeast-striking fault in Page Sandstone. Its polished surface strikes N55°E, dips 60°W, and displays grooves raking 20–30°SW. The geometry again indicates reverse-right-lateral slip. This outcrop marks the north end of a lineation traceable on topographic maps and air photos for at least 4 km toward S40°W into gently dipping Navajo Sandstone. The fault-controlled lineation and preserved fault surface occupy the upper Navajo and Page Sandstones, and the Jurassic Carmel through Cretaceous Wahweap Formations immediately to the east form another broad, z-shaped bend in the trace of the monocline.

As a whole, the map- and outcrop-scale faulting in Domain 1 defines a narrow, monocline-parallel zone of intense deformation which constitutes a shear zone. From the north to the south end of Domain 1 the shear zone occupies progressively lower stratigraphic intervals within steeply east-dipping beds. Fault and

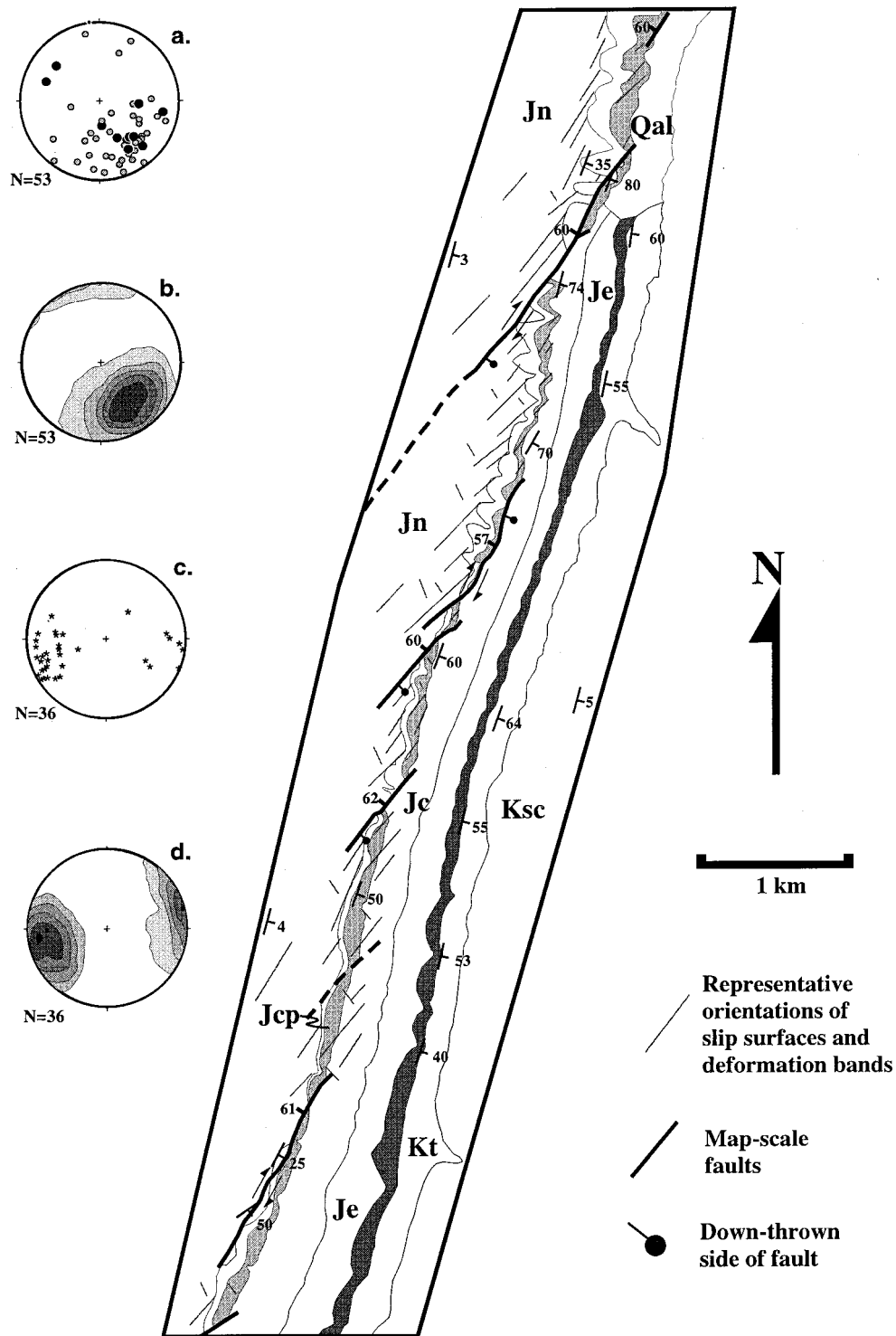


Fig. 8. Geology of Domain 2. northeast-striking, northwest-dipping faults offset the Page Sandstone (light shading) in reverse-right-lateral fashion. Dakota Sandstone, intensely faulted in Domain 1, is unaffected by faulting in Domain 2. Representative orientations of slip surfaces and deformation bands depict structural features too small to show at map-scale. (a) Equal-area plot of poles to faults (black) and slip surfaces (grey). (b) Kamb contour plot of poles illustrates tight clustering of northeast-striking, northwest-dipping fault and slip surface orientations. (c) Equal area plot and (d) Kamb contour plot of slickenline orientations. Slickenlines plunge gently toward the southwest, disclosing reverse-right-lateral slip on northeast-striking, west-dipping faults.

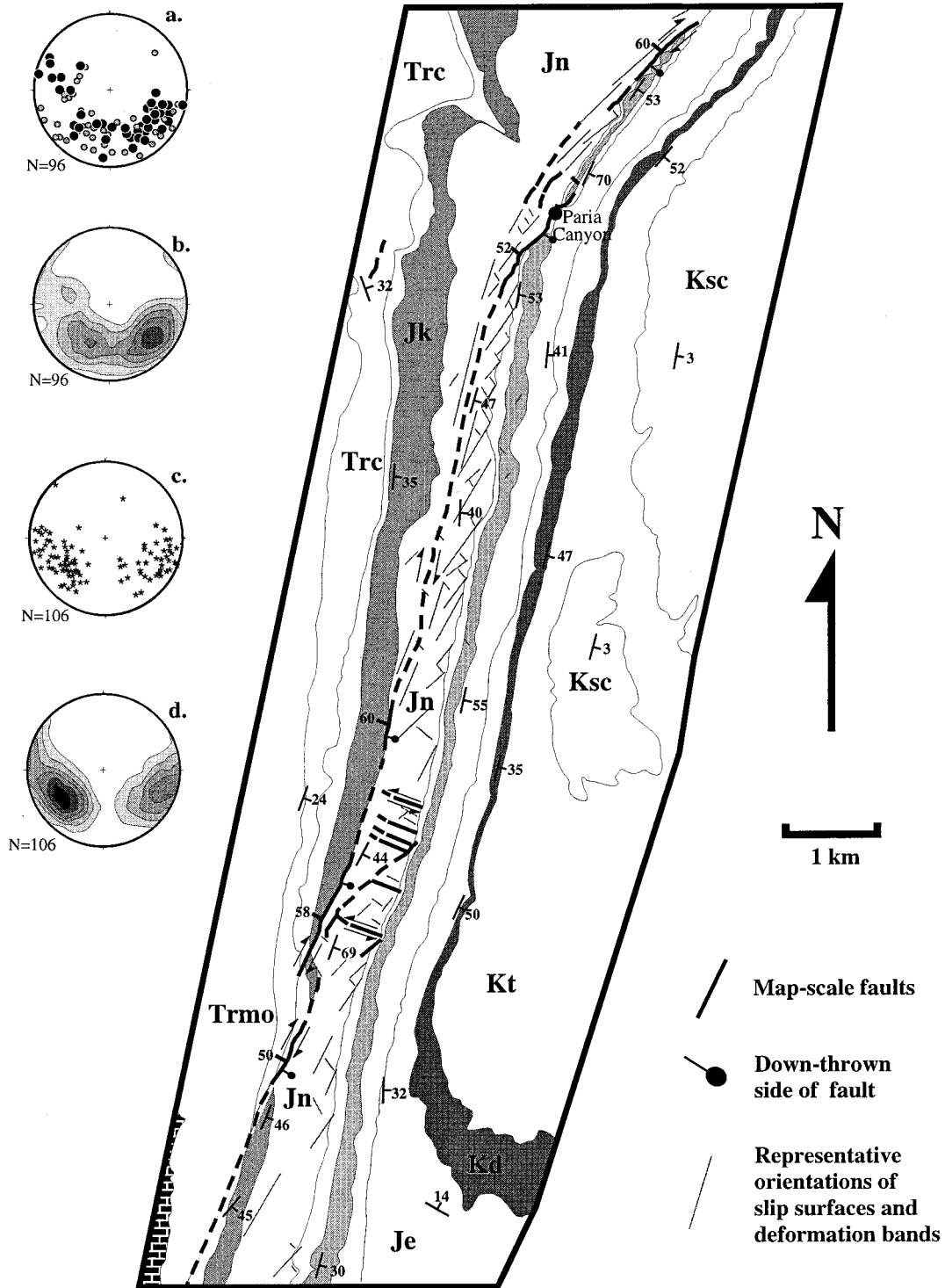


Fig. 9. Geology of Domain 3. Linear valleys, gouge, breccia, and exposures of polished fault surfaces reveal long, continuous faulting in Navajo and Kayenta Formations. Slip surfaces and deformation bands occupy both northeast-striking and northwest-striking orientations. (a) Equal-area plot of poles to faults (black) and slip surfaces (grey). (b) Kamb contour plot of poles to faults and slip surfaces, showing a primary set of northeast-striking, northwest-dipping surfaces and a secondary set of northwest-striking, northeast-dipping surfaces. (c) Equal-area plot of slickenline orientations. (d) Kamb contour plot of slickenline orientations. Southwest-plunging slickenlines lie on northeast-striking faults, and south-east-plunging slickenlines lie on northwest-striking faults.

slickenline orientations at the north and south ends of Domain 1 indicate a large ratio (up to 5:1) of right-lateral strike-slip to dip-slip offset across the long, northeast-striking, west-dipping faults; the northwest-striking faults between Grosvenor's Arch and Pump Canyon Spring also record a 5:1 ratio of left-slip to reverse-slip. Although slickenlines typically preserve only the latest slip vector on a fault surface, the observed orientations along this 15 km stretch of the monocline are consistent with interpretation as synthetic (northeast-striking) and antithetic (northwest-striking) conjugates in a zone of oblique (i.e. reverse right-lateral) displacement.

3.2. Domain 2

Structural Domain 2 begins immediately south of the northeast-striking fault surface at the southern end of Domain 1 (Fig. 8). This 12 km-long interval is marked by several map-scale northeast-striking faults in the lower Carmel Formation, Page Sandstone, and upper Navajo Sandstone; the deformation is in a slightly lower stratigraphic interval. Map-scale faults in Domain 2 have trace lengths on the order of 1 km. Map view reveals apparent right-lateral offset on the order of tens to a few hundred meters, and where canyons incise the faults their reverse separation is evident. Average orientation of the northeast-striking faults in Domain 2 is $N41^{\circ}E$, $46^{\circ}NW$, again with slickenlines raking about $30^{\circ}SW$. These faults are similar in orientation to those found at the north end of Domain 1 and between Domains 1 and 2, but with shorter trace lengths and offset on the order of only a few meters to tens of meters.

At outcrop-scale, the Page and Navajo Sandstones in Domain 2 are intensely fractured. Minor fault surfaces (slip surfaces) and deformation bands show two primary orientations: a prominent northeast-striking, northwest-dipping set and a secondary northwest-striking, northeast-dipping set (Fig. 8). Deformation in Domain 2 is still consistent with the interpretation as a reverse-right-lateral shear zone, but long, en échelon synthetic faults rather than short, closely spaced antithetic faults dominate Domain 2.

3.3. Domain 3

Domain 3 begins at Paria Canyon, and is distinguished by evidence for continuous, through-going faulting in the Navajo Sandstone and Kayenta Formation (Fig. 9). The mouth of Paria Canyon exposes a northeast-striking, northwest-dipping fault surface similar to the one at the boundary between Domains 1 and 2, again with slickenlines and grooves that rake $30^{\circ}SW$. The cross-sectional view at the mouth of the canyon reveals Navajo and Page



Fig. 10. North-directed photograph of the northeast-striking, northwest-dipping fault surface at the mouth of Paria Canyon. Page Sandstone member of the Carmel Formation on the hanging wall lies in fault contact above stratigraphically higher Carmel Formation redbeds. Stratigraphic relationship and drag folding in Carmel redbeds indicate a reverse component of faulting. Slickenlines on the fault surface (not visible) rake $20\text{--}30^{\circ}SW$, disclosing a significant right-lateral component of slip. Geologist is Bill Abbey.

Sandstones in the hanging wall, above reverse drag-folded Carmel Formation redbeds in the footwall (Fig. 10). Jurassic Entrada Sandstone through Cretaceous Wahweap Formation east of the fault surface (up-section) again form a broad, z-shaped fold in map view. The fault surface exposed at Paria Canyon marks the north end of a series of linear valleys which trend $S20^{\circ}W$ across $N10^{\circ}E$ -striking, steeply east-dipping Navajo Sandstone. Evidence for through-going faulting is found in the valleys as fault gouge and breccia, intensely fractured Navajo Sandstone, and several exposures of northeast-striking, steeply west-dipping polished fault surfaces. Because the strike of the fault zone nearly parallels the strike of bedding in the Navajo, the zone of deformation crosses the Navajo Sandstone at a very low angle; the steeply west-dipping fault requires 8 km of strike length to cross the (approximately) 400 m thick, east-dipping sandstone. As a result of this geometry, a large amount of right lateral displacement across the fault zone is theoretically possible without causing a noticeable disruption of the surface trace of the Navajo Sandstone. Map-scale fault surfaces measured in the Navajo in Domain 3 yield an average orientation of $N36^{\circ}E$, $59^{\circ}NW$, with slickenlines raking $30^{\circ}SW$. At the south end of Domain 3 the fault zone offsets Triassic/Jurassic Kayenta and Triassic Moenave Formations, in an apparent right-lateral fashion, on the east side of Fivemile Valley before it disappears beneath alluvium and colluvium on the valley floor.

Although at map scale northeast-striking (synthetic)

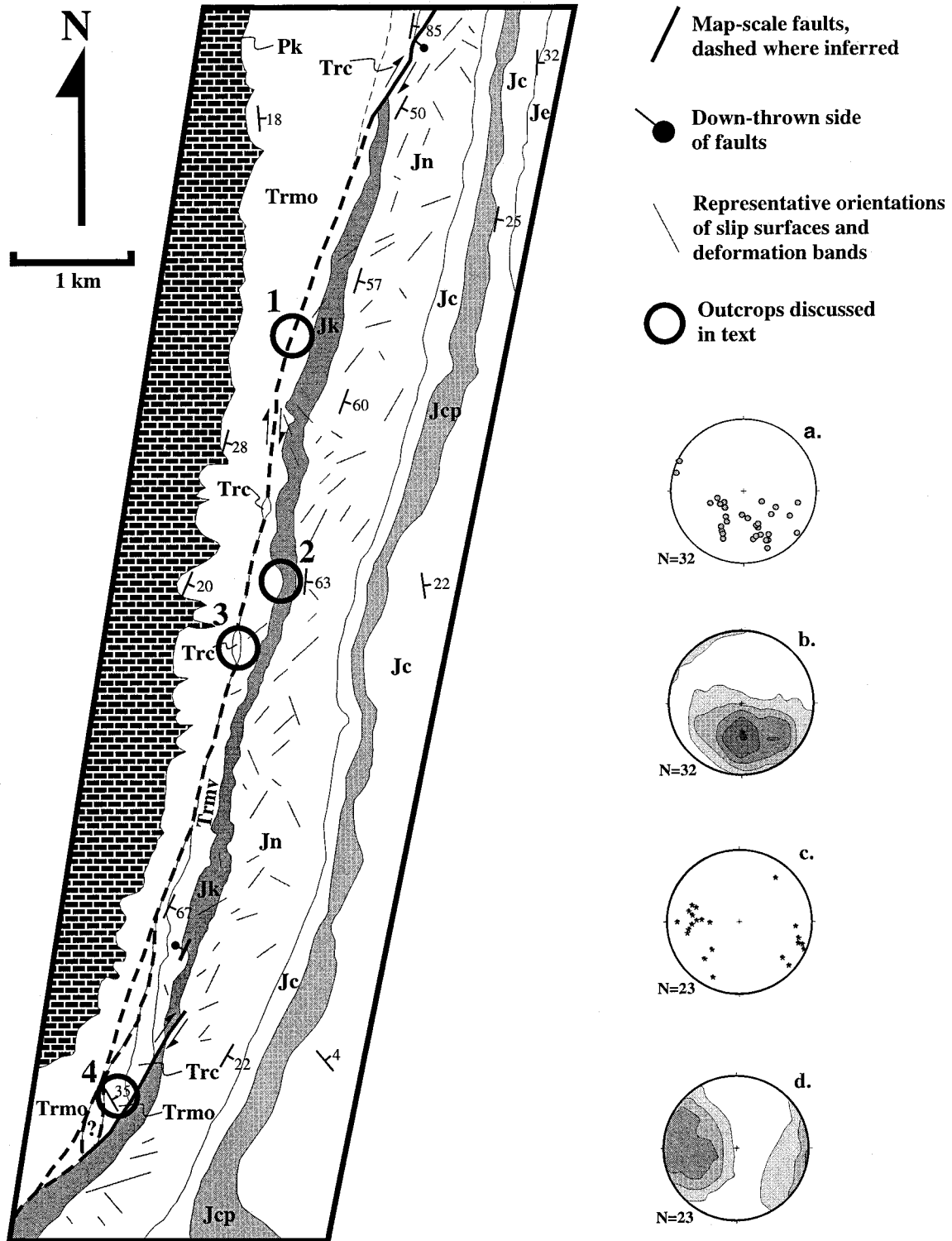


Fig. 11. Geology of Domain 4. Through-going faulting is inferred based on four key outcrops described in the text (locations circled). Intense deformation is obscured by alluvium in the valley, formed by Moenkopi and Chinle Formation shales. (a) Equal-area plot and (b) Kamb contour plot of poles to slip surfaces in Navajo, Kayenta, and Moenave Formations. (c) Equal-area and (d) Kamb contour plot of slickenline orientations.

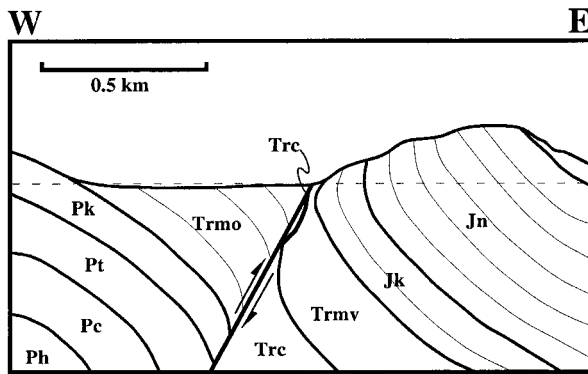


Fig. 12. Cross-sectional sketch based on outcrops visible in the canyon at Location 2 (above dashed line) and inferred subsurface structure (below dashed line). The inferred west-dipping fault with reverse separation accounts for overturned bedding at Location 2 and the apparent absence of Chinle Formation in this part of Domain 4. The sliver of Chinle Formation shown in the sketch just below the surface is a reverse- (and right-lateral?) fault-bounded block caught in the shear zone, representing the relationship exposed at Location 3.

faults are prevalent in Domain 3, a few short north-west-striking, northeast-dipping faults similar to those found in Domain 1 offset the Navajo Sandstone east of the through-going synthetic faults. These antithetic faults accommodate meters to tens of meters of reverse-left-lateral offset within the Navajo Sandstone. Oblique slip is expressed by slickenlines that rake 18° E. Outcrop-scale deformation bands and slip surfaces also show a bimodal distribution of synthetic and antithetic orientations (Fig. 9). Deformation in Domain 3 is concentrated in the Navajo Sandstone, with some fracturing and deformation bands affecting the Page Sandstone; however, no map-scale faults offset the Page Sandstone south of Paria Canyon. The most intense deformation has again moved stratigraphically down-section, from the interval of upper Navajo/Page/Carmel Formations in Domain 2 into the Kayenta/Navajo Formations within Domain 3.

3.4. Domain 4

In Domain 4 the shear zone lies southward and down-section in the Triassic Chinle and Moenkopi Formations in Fivemile Valley (Fig. 11). These shaley Triassic units are sandwiched between resistant Permian Kaibab Limestone on the west side of the valley, dipping $25\text{--}35^{\circ}$ east, and a ridge of $65\text{--}85^{\circ}$ east-dipping Moenave, Kayenta, and Navajo Sandstones on the east side. Most evidence for the continuation of the shear zone is hidden beneath alluvium and colluvium on the valley floor, but a few key outcrops allow it to be traced southward almost to the Utah–Arizona border.

Location 1 is a northeast-striking, steeply west-dipping, remarkably planar slope of Navajo, Kayenta,

and Moenave Formations along strike with the linear valleys described in Domain 3. Near the base of the slope, a sliver of Triassic Moenkopi Formation shale several tens of meters long rests against Triassic Moenave sandstone; the Triassic Chinle Formation, which should separate the two, is missing. This older-on-younger relationship could be produced by faulting with a reverse component of offset.

The exposure of interest at Location 2 follows a drainage that provides a transect into the ridge of Moenave, Kayenta, and Navajo Formations on the east side of Fivemile Valley (Fig. 12). Near the mouth of the wash, several outcrops of overturned Moenave Formation beds are visible, striking $N15^{\circ}$ E and dipping 52° NW. Towards the east, along the wash, dips gradually steepen to vertical over the course of tens of meters in Moenave and Kayenta Formations. Within 200 m of the overturned outcrops, at the mouth of the wash, bedding is upright, striking $N10^{\circ}$ E and dipping 65° SE. The attitudes describe an overturned syncline that may be the result of drag folding of beds immediately in the footwall of the shear zone assumed to lie beneath alluvium on the valley floor.

At Location 3, an isolated hill of northwest-striking, steeply east-dipping sandstone and conglomerate of the Chinle Formation (Shinarump Member) protrudes from the valley floor. Triassic Moenave sandstone and shale on the east side of the valley, only a few tens of meters away, strike northeast. Triassic Moenkopi and Permian Kaibab Formations on the west side of the valley also strike northeast. A northeast-striking, near-vertical fault surface with southwest-raking slickenlines is preserved in the isolated Shinarump sandstone block. The outcrop is likely a sliver of Chinle Formation caught in the fault zone, which itself is obscured on the valley floor.

Evidence for faulting at Location 4 is similar to that at Location 3. A wedge of distinctively striped Moenkopi shale striking northwest is truncated at its southern edge by a ridge of Kayenta Formation striking northeast; Chinle Formation is absent between the two. Like the Chinle ridge at Location 2, the wedge of strangely oriented Moenkopi Formation here may be a sliver of material caught in a reverse fault zone. The fault contact between the two units is evident and the missing stratigraphic section discloses at least a reverse component of offset; a right-lateral component also may be present. These outcrops make it possible to track the presence of the shear zone almost to the Utah–Arizona border, south of which exposure is completely obscured by alluvium.

4. Summary of field observations

In southern Utah the steep, east-dipping limb of

SUMMARY OF OBSERVATIONS

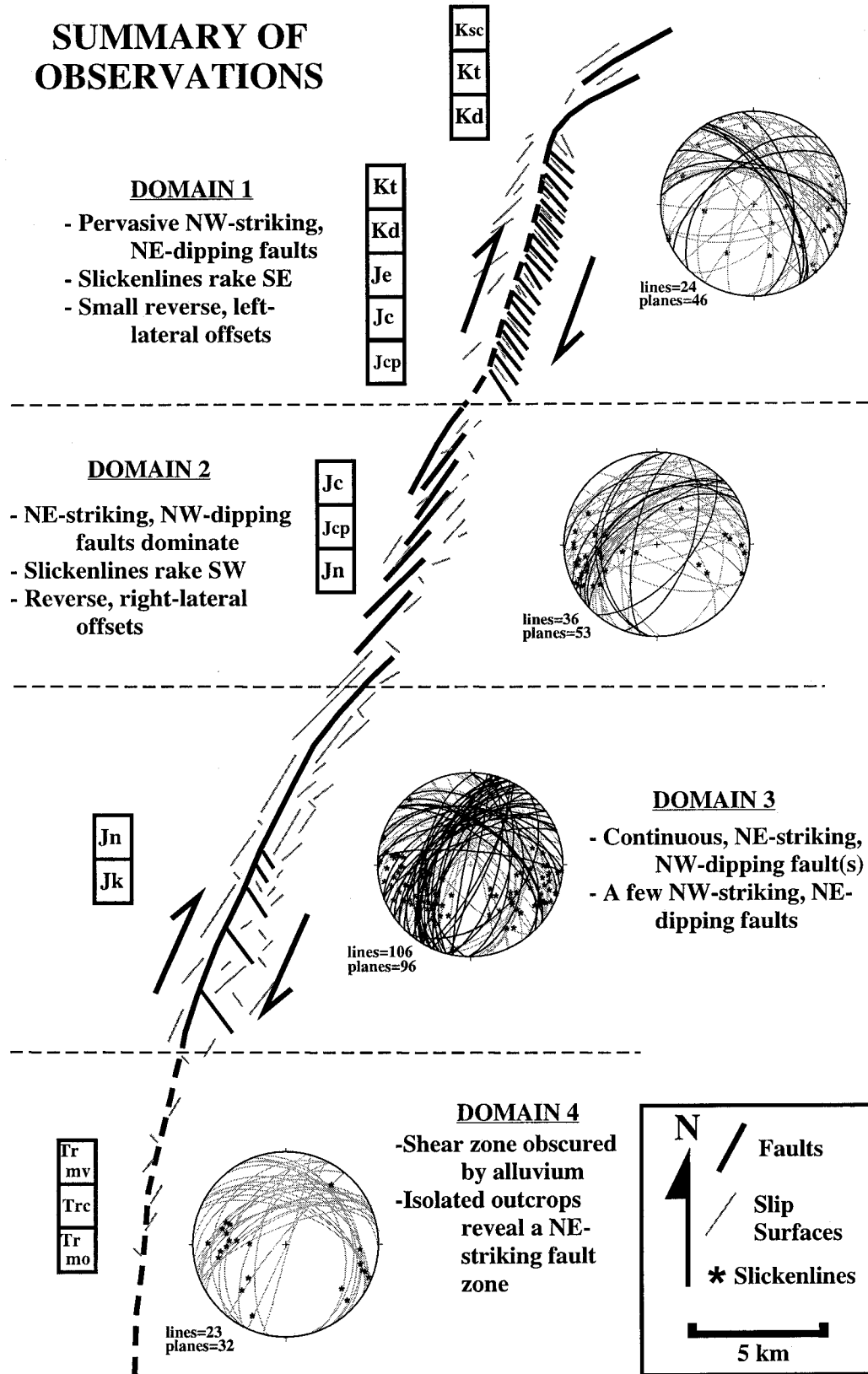


Fig. 13. Summary of structural and stratigraphic evidence for an oblique shear zone on the steep limb of the East Kaibab monocline. Progressively higher stratigraphic intervals are affected by intense deformation from south to north, and structural style changes from continuous, through-going faulting in the south to disjointed but pervasive fractures northward. Along the entire shear zone, northeast-striking, northwest-dipping synthetic faults accommodate reverse-right-lateral slip, and northwest-striking, northeast-dipping antithetic faults accommodate reverse-left-lateral slip. The progression in structural style and stratigraphic level combined with consistent slip indicators suggests transpressive fault-propagation folding.

the East Kaibab monocline hosts a narrow zone of intense deformation marked by pervasive map-scale and outcrop-scale faulting. This 'shear zone' is seen to move progressively down-section through steep, east-dipping Mesozoic strata from north to south, and the character of deformation changes with each new stratigraphic interval affected (Fig. 13). At the northern termination of Domain 1, northeast-striking, steeply west-dipping faults offset Jurassic Carmel through Cretaceous Straight Cliffs Formations in reverse-right-lateral fashion. Slickenlines on fault surfaces rake 15–20°SW. Cretaceous Wahweap and Kaiparowits Formations east of (and stratigraphically above) these faults are bent in map view into a broad, z-shaped fold.

Domain 1 deformation occupies a slightly lower stratigraphic interval: Jurassic Page Sandstone through Cretaceous Tropic Shale. Northwest-striking, north-east-dipping faults with 20°SE-raking slickenlines accommodate reverse-left-lateral offset and clockwise rotation of intervening strata. Faults lie in a right-stepping en échelon pattern and define a narrow deformation zone that trends N20°E, parallel to the trend of the monocline.

Between Domains 1 and 2 another long, northeast-striking fault lies just west of (and stratigraphically below) a broad, z-shaped bend in steeply east-dipping Jurassic and Cretaceous strata. Southward, deformation in Domain 2 affects the upper Navajo Sandstone, Page Sandstone, and Carmel Formation redbeds. Map- and outcrop-scale, northeast-striking, steeply west-dipping faults accommodate reverse-right-lateral displacement of intervening strata. Slickenline orientations on large fault surfaces average 30°SW, implying a 3:1 ratio of strike-slip to dip-slip on the northeast-striking faults. Domain 2 faults are left-stepping and slightly oblique to the trend of the monocline, but again define a N20°E-trending, monocline-parallel zone of deformation.

Beyond yet another prominent northeast-striking fault surface and z-shaped bend at the southern end of Domain 2, Domains 3 and 4 display evidence for reverse-right-lateral displacement on a single northeast-striking, west-dipping fault or series of long, continuous relay faults. In Domain 3 intense deformation is concentrated in the Navajo Sandstone and Kayenta Formation. Major fault surfaces have an average strike and dip of N36°E, 59°NW with southwest-raking slickenlines. Evidence for continuous, through-going faulting continues to the south in Domain 4, moving down-section into the Triassic Moenave, Chinle, and Moenkopi Formations. Outcrops in these valley-forming shales are scarce, but several key exposures reveal the presence of a northeast-striking fault with at least a reverse component of separation.

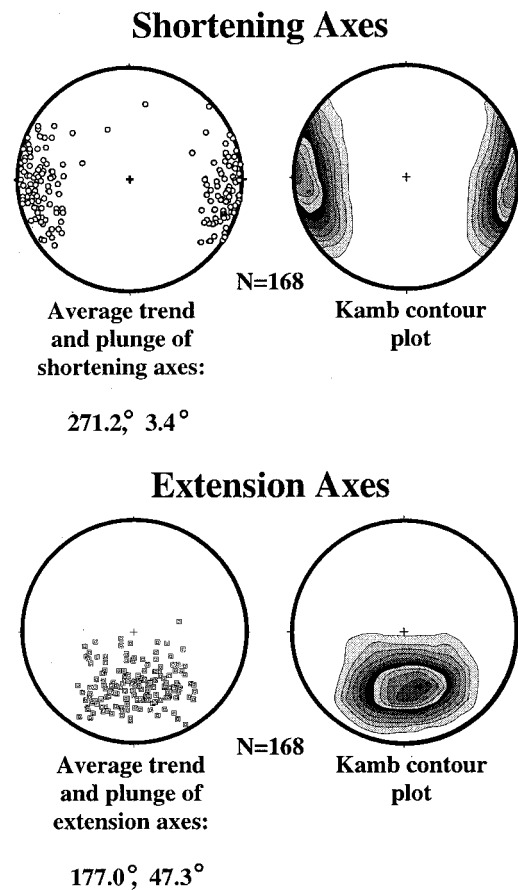


Fig. 14. Equal-area and Kamb contour plots of shortening (S_3) and extension (S_1) axes calculated for 168 faults and slip surfaces using the kinematic analysis described by Marrett and Allmendinger (1990). The average shortening axis is consistent with ENE–WNW horizontal compression, and the orientation of the extension axis indicates reverse-right-lateral slip given a N20°E-trending shear zone (the trend of the East Kaibab monocline).

5. Discussion

The continuous, narrow zone of deformation described above is interpreted as a brittle to semi-brittle shear zone occupying the steep limb of the East Kaibab monocline. Northeast-striking faults are synthetic to an overall reverse-right-lateral sense of shear, and northwest-striking faults are antithetic to the shear zone. The orientation and sense of offset on map-scale and outcrop-scale structures are consistent with a reverse-right-lateral sense of shear for at least the northernmost 50 km of the monocline. Although slickenline orientations typically record the slip vector of only the latest episode of movement on a fault, the close agreement of fault attitudes and slickenline orientations observed at map and outcrop-scale over a full 50 km distance strengthens the argument that a right-lateral component of slip operated throughout shear zone development.

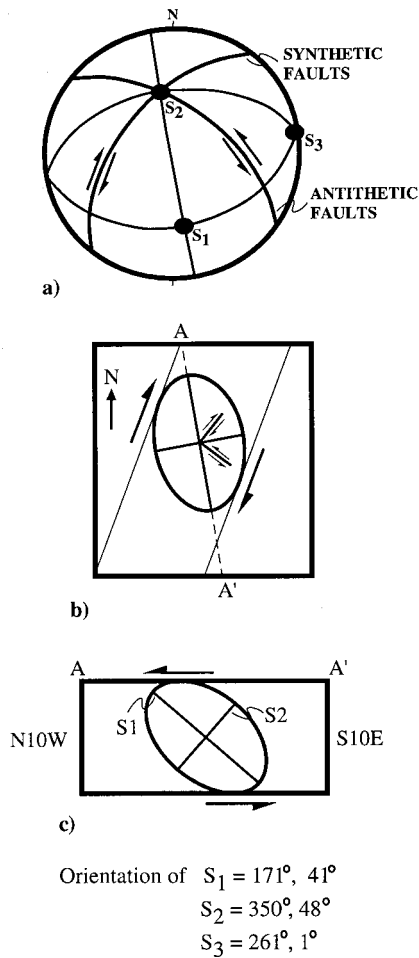


Fig. 15. (a) Lower-hemisphere equal-area projection showing the orientations of maximum, minimum, and intermediate stretch axes (S_1 , S_3 , and S_2 , respectively) and principal planes for a finite strain ellipsoid in the shear zone. Axes were calculated from average orientations of synthetic and antithetic faults. (b) Map-view projection of a strain ellipsoid with the calculated S_1 and S_3 orientations within a $N20^\circ E$ -trending shear zone. Map traces of synthetic and antithetic faults are shown. Relative lengths of S_1 and S_3 axes have not been calculated, but the orientation of the horizontal strain ellipse shows right-handed shear. (c) Cross-section view of the strain ellipsoid along $A-A'$, parallel to the S_1-S_2 plane. Orientation of the S_1 axis with respect to the shear zone displays reverse, right-lateral shear.

Fault-slip data were used to calculate the orientations of shortening and extension axes using the method described by Marrett and Allmendinger (1990). East Kaibab monocline fault-slip data included strike and dip of fault and slip surfaces, rake of slickenlines (representing the slip vector), and sense of slip. Shortening and extension axes were calculated for each of 168 faults for which all of the above information was known. Orientations and Kamb contour plots of the axes are shown in Fig. 14. The average shortening axis trends 271.2° and plunges 3.4° , and the average extension axis plunges 47.3° toward 177.0° . The near-horizontal, east–west orientation of the shortening axis is consistent with Laramide, ENE-directed, compres-

sive stress determined by Reches (1978) and Anderson and Barnhard (1986).

Attitudes of synthetic and antithetic faults within the shear zone were used to determine the orientation of the finite strain ellipsoid. Three assumptions were made concerning fault geometry: first, that the line of intersection of synthetic and antithetic faults is the intermediate stretch axis (S_2) of the ellipsoid; second, that the S_2-S_3 plane bisects the acute angle between the fault sets; and third, that faults did not rotate considerably during progressive deformation. Based on these assumptions, orientations of the principal axes of the finite strain ellipsoid in the deformed zone are (trend, plunge): $171, 41$ (S_1); $261, 1$ (S_3); and $350, 48$ (S_2) (Fig. 15). These values are remarkably similar to the shortening (S_3) and extension (S_1) directions found using the Marrett and Allmendinger method. The geometric solution also yields a minimum stretch (maximum shortening) axis that is horizontal with an ENE trend, generally parallel to the direction of Laramide contraction. Although the relative magnitudes of the stretch axes have not been determined, the orientation of S_1 implies reverse-right-lateral offset across the zone. The sense of offset indicated by the strain ellipsoid is consistent with the sense of offset demonstrated by slickenline orientations observed on fault surfaces, which themselves imply a ratio of up to 5:1 of right-lateral slip to reverse slip across the shear zone.

Despite the similarity in fault and slickenline orientations along the northern 50 km of the East Kaibab monocline, deformation mechanisms are partitioned from one domain to the next. At map scale, en échelon antithetic faults are favored in Domain 1, en échelon synthetic faults dominate Domain 2, and through-going faulting is preferred in Domains 3 and 4. The reasons for the changes in style are unclear. Different structures may result from different mechanical responses of the stratigraphic intervals involved, since both structural style and stratigraphic interval change from north to south. It is also possible that the changes are related to structural position within the fold. The slight northward plunge of the monocline creates an extremely elongated down-plunge view of deformation, such that each step towards the southwest exposes a deeper structural level, closer to the basement fault. Considered in this way, it is relevant that evidence for through-going faulting is present in the structurally lower southern part of the study area but gives way to more distributed deformation towards the north, at higher structural levels. The progression from continuous faulting at depth to distributed fracturing at shallower levels is consistent with fault-propagation folding (Suppe and Medwedeff, 1984; Suppe, 1985; Jamison, 1987; Erslev, 1991). In the case of the East Kaibab monocline, basement-rooted faulting has propagated upward through Paleozoic and

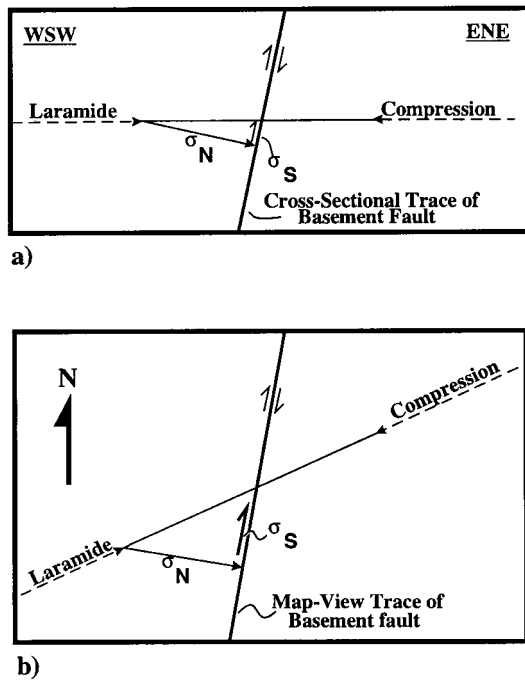


Fig. 16. The apparent difficulty of reactivating a steeply dipping basement fault with Laramide horizontal compressive stress as seen in cross-section (a) largely disappears when the perspective changes to map-view (b). An ENE-directed horizontal stress is ideally directed to cause right-lateral reactivation of a $N10^{\circ}$ – 20° E-striking, steeply dipping basement fault such as the one underlying the East Kaibab monocline.

Mesozoic strata to the level of the Navajo Sandstone. En échelon faults in Domains 1 and 2 may represent fractures immediately ahead of the propagating fault tip which would have joined and extended the basement-rooted fault if deformation had continued. In the down-plunge perspective provided by the map, these fractures are exposed over a distance of 25–30 km, whereas in vertical cross-section they would occupy a stratigraphic thickness of less than 1500 m, possibly making them difficult to recognize and measure.

The down-plunge view of the monocline and shear zone exposed in southern Utah invites interpretation of the East Kaibab monocline as a basement-rooted fault-propagation fold. Grand Canyon exposures show that the fold form of the monocline widens upward from basement, consistent with trishear fault-propagation fold models (Erslev, 1991). However, the brittle shear zone exposed along the steep limb in southern Utah remains narrow as it propagates up-section through the steep limb of the fold. The shear zone represents a frozen moment in the progressive development of fault and fold: it preserves intense deformation that formed directly ahead of the fault tip as the propagating fault overtook the developing fold. The right-lateral component of slip in the shear zone is probably tied to Laramide right-lateral displacement

on the underlying basement fault. Thus the origin of the East Kaibab monocline should be considered in the context of transpressional fault-propagation folding rather than reverse-slip drape folding.

The regional tectonic implications of these findings are significant. Literature on Colorado Plateau monoclines has commonly emphasized the role of reverse-slip reactivation of Precambrian fault zones (e.g. Huntoon and Sears, 1975; Davis, 1978; Huntoon, 1993). However, as seen in cross-section, a horizontal compressive stress acting *perpendicular* to a near-vertical fault results in a high magnitude of normal stress on the fault plane, making reverse reactivation difficult to achieve. This limitation largely disappears when the perspective of viewing changes from cross-sectional to map view (Fig. 16). A northeasterly directed horizontal compressive stress acting on a $N20^{\circ}$ E-striking, steeply west-dipping Precambrian fault is suited ideally to reactivating the fault in a right-handed strike-slip fashion, with a component of reverse motion resulting from the steep westward dip of the fault. This is what we believe has occurred along at least the northern 50 km of the East Kaibab monocline, and possibly across other basement-cored uplifts with structural trends oblique to the regional shortening direction.

6. Conclusions

A long, narrow zone of concentrated map-scale and outcrop-scale faulting defines a brittle to semi-brittle shear zone on the steep limb of the East Kaibab monocline. The character of deformation in the shear zone varies from south to north: through-going faulting offsets older strata at the south end of the study area, and more distributed, discontinuous deformation affects progressively younger strata to the north. A down-plunge view of the northern 50 km of the north-plunging monocline resembles a fault-propagation fold in which the discrete fault rupture has propagated through Triassic strata into Jurassic Navajo Sandstone. Intense deformation directly ahead of the fault tip is seen in stratigraphically higher Jurassic and Cretaceous strata. The orientations of fault surfaces exposed in the southern part of the study area closely parallel the orientation of the underlying basement fault exposed in the Grand Canyon, leading to the assumption that the shear zone roots into the basement fault.

Orientations of faults and slickenlines within the shear zone record at least a late-stage episode of reverse-right-lateral slip. Northeast-striking and northwest-striking faults are interpreted as synthetic and antithetic, respectively, to a $N20^{\circ}$ E-striking, steeply west-dipping shear zone, parallel to both the monocline and the Grand Canyon exposure of the under-

lying basement fault. Inversion of fault and slickenline data yields a finite strain ellipsoid with an orientation consistent with reverse-right-lateral slip. The maximum shortening axis of the ellipsoid coincides with the northeast-directed horizontal compressive stress determined for Laramide deformation on the Colorado Plateau.

Oblique displacement in the shear zone involved a ratio of up to 5:1, strike-slip to dip-slip. If this ratio characterizes the slip vector throughout formation of the monocline (during initial folding and late-stage faulting in Mesozoic strata), the observed structural relief of 1600 m would correspond to a right-lateral offset of up to 8000 m between the structural crest of the Kaibab Uplift and the adjacent Kaiparowits Basin.

Acknowledgements

We acknowledge the valuable input received from Charles F. Kluth and William G. Higgs, both of Chevron, Inc., with whom we discussed map relationships early in the project. Conversations with the structural geologists at Mobil Oil in Dallas, TX were instrumental in clarifying many of the concepts presented here. We gratefully acknowledge the field assistance and input provided by Seth Gering, Shari Christofferson, Danielle Vanderhorst, Pilar Garcia, William Abbey, and Jessica Greybill. Thanks to Karl Karlstrom, Ken McClay, Richard Allmendinger, Don Fisher, and Scott Wilkerson for valuable input on early versions of the manuscript. Field work was supported through funding by the National Science Foundation, namely through NSF#EAR-9406208.

References

- Anderson, R.E., Barnhard, T.P., 1986. Genetic relationship between faults and folds and determination of Laramide and neotectonic paleostress, western Colorado Plateau-Transition Zone, central Utah. *Tectonics* 5, 335–357.
- Babenroth, D.L., Strahler, A.N., 1945. Geomorphology and structure of the East Kaibab monocline, Arizona and Utah. *Geological Society of America Bulletin* 56, 107–150.
- Barnes, C.W., 1974. Interference and gravity tectonics in the Gray Mountain area, Arizona. In: Karlstrom, T.N.V., Swann, G.A., Eastwood, R.L. (Eds.), *Geology of Northern Arizona with Notes on Archaeology and Paleoclimate—Part 2, Area Studies and Field Studies*. Geological Society of America Rocky Mountain Section, pp. 442–453.
- Barnes, C.W., 1987. Geology of the Gray Mountain area, Arizona. In: Beus, S.S. (Ed.), *Geological Society of America Centennial Field Guide*, 6. Geological Society of America, pp. 379–384.
- Bowers, W.E., 1972. The Canaan Peak, Pine Hollow and Wasatch Formations in the Table Cliffs region, Garfield County, Utah, Bulletin 1331-B. United States Geological Survey.
- Chapin, C.E., Cather, S.M., 1983. Eocene tectonics and sedimentation in the Colorado Plateau–Rocky Mountain area. In: Lowell, J.D., Gries, R. (Eds.), *Rocky Mountain Foreland Basins and Uplifts*. Rocky Mountain Association of Geologists, pp. 33–56.
- Davis, G.H., 1978. Monocline fold pattern of the Colorado Plateau. In: Matthews, V. (Ed.), *Laramide Folding Associated with Basement Block Faulting in the Western United States*, Memoir 151. Geological Society of America, pp. 15–233.
- Dutton, C.E., 1882. Tertiary History of the Grand Canyon District, Monograph 2. United States Geological Survey.
- Erslev, E.A., 1991. Trishear fault-propagation folding. *Geology* 19, 617–620.
- Erslev, E.A., Rogers, J.L., 1993. Basement–cover geometry of Laramide fault-propagation folds. In: Schmidt, C.J., Chase, R.B., Erslev, E.A. (Eds.), *Laramide Basement Deformation in the Rocky Mountain Foreland of the Western United States*, Special Paper 280. Geological Society of America, pp. 125–146.
- Gregory, H.E., Moore, R.C., 1931. The Kaiparowits region: a geographic and geological reconnaissance of parts of Utah and Arizona, Professional Paper 164. United States Geological Survey.
- Hintze, L.F., 1988. Geologic History of Utah. Brigham Young University Geology Studies Special Publication 7.
- Huntoon, P.W., 1969. Recurrent movements and contrary bending along the West Kaibab fault zone. *Plateau* 42, 66–74.
- Huntoon, P.W., 1971. The deep structure of the monoclines in eastern Grand Canyon, Arizona. *Plateau* 43, 148–158.
- Huntoon, P.W., 1974. Synopsis of Laramide and post-Laramide structural geology of the eastern Grand Canyon, Arizona. In: Eastwood, R.L., Karlstrom, T.N.V., Swann, G.A. (Eds.), *Geology of Northern Arizona, Part 1—Regional Studies*. Northern Arizona University, Flagstaff, Arizona, pp. 317–335.
- Huntoon, P.W., 1981. Grand Canyon monoclines; vertical uplift or horizontal compression? In: Boyd, D.W., Lillegraven, J.A. (Eds.), *Rocky Mountain Foreland Basement Tectonics*, 19. University of Wyoming Contributions to Geology, pp. 127–134.
- Huntoon, P.W., 1993. Influence of inherited Precambrian basement structure on the localization and form of Laramide monoclines, Grand Canyon, Arizona. In: Schmidt, C.J., Chase, R.B., Erslev, E.A. (Eds.), *Laramide Basement Deformation in the Rocky Mountain Foreland of the Western United States*, Special Paper 280. Geological Society of America, pp. 243–256.
- Huntoon, P.W., Sears, J.W., 1975. Bright Angel and Eminence Faults, eastern Grand Canyon, Arizona. *Geological Society of America Bulletin* 86, 465–472.
- Huntoon, P.W., Billingsley, G.H., Sears, J.W., Ilg, B.R., Karlstrom, K.E., Williams, M.L., Hawkins, D., Breed, W.J., Ford, T.D., Clark, M.D., Babcock, R.S., Brown, E.H., 1996. Geologic map of the eastern part of the Grand Canyon National Park, Arizona. Grand Canyon Association.
- Jamison, W.R., 1987. Geometric analysis of fold development in overthrust terranes. *Journal of Structural Geology* 9, 207–220.
- Karlstrom, K.E., Daniel, C.G., 1993. Restoration of Laramide right-lateral strike slip in northern New Mexico by using Proterozoic piercing points: tectonic implications from the Proterozoic to the Cenozoic. *Geology* 21, 1139–1142.
- Marrett, R., Allmendinger, R.W., 1990. Kinematic analysis of fault-slip data. *Journal of Structural Geology* 12, 973–986.
- Maxson, J.H., 1961. Geologic map of the Bright Angel quadrangle, Grand Canyon National Park, Arizona. Grand Canyon Natural History Association.
- Mitra, S., Mount, V.S., 1998. Foreland basement-involved structures. *American Association of Petroleum Geologists Bulletin* 82, 70–109.
- Ohlman, J.R., 1982. A structural analysis of the Butte–Eminence fault system, eastern Grand Canyon, Coconino County, Arizona. MSc thesis, Northern Arizona University.
- Powell, J.W., 1873. Exploration of the Colorado River of the West

- and its Tributaries Explored in 1869–1872. Smithsonian Institution, Washington, DC.
- Prucha, J.J., Graham, J.A., Nickelsen, R.P., 1965. Basement-controlled deformation in Wyoming province of Rocky Mountain Foreland. *American Association of Petroleum Geologists Bulletin* 49, 966–992.
- Reches, Z., 1978. Development of monoclines: Part I, structure of the Palisades Creek branch of the East Kaibab monocline, Grand Canyon, Arizona. In: Matthews, V. (Ed.), *Laramide Folding Associated with Basement Block Faulting in the Western United States*, Memoir 151. Geological Society of America, pp. 235–273.
- Reches, Z., Johnson, A.M., 1978. Development of monoclines: Part II, theoretical analysis of monoclines. In: Matthews, V. (Ed.), *Laramide Folding Associated with Basement Block Faulting in the Western United States*, Memoir 151. Geological Society of America, pp. 273–311.
- Sanford, A.R., 1959. Analytical and experimental study of simple geologic structures. *Geological Society of America Bulletin* 70, 19–52.
- Sargent, K.A., Hansen, S.E., 1982. Bedrock geologic map of the Kaiparowits coal-basin area, Utah. United States Geological Survey Miscellaneous Investigations Map I-1033-I.
- Stearns, D.W., 1971. Mechanisms of drape folding in the Wyoming Province. In: Renfro, A.R. (Ed.), *Symposium on Wyoming Tectonics and Their Economic Significance*. 23rd Field Conference Guidebook. Wyoming Geological Association, pp. 125–143.
- Stearns, D.W., 1978. Faulting and forced folding in the Rocky Mountain foreland. In: Matthews, V. (Ed.), *Laramide Folding Associated with Basement Block Faulting in the Western United States*, Memoir 151. Geological Society of America, pp. 1–38.
- Stern, S., 1992. Geometry of Basement Faults Underlying the Northern Extent of the East Kaibab Monocline, Utah. MSc thesis, University of North Carolina at Chapel Hill.
- Stone, D.S., 1969. Wrench faulting and Rocky Mountain tectonics. *The Mountain Geologist* 6, 67–79.
- Stone, D.S., 1984. The Rattlesnake Mountain, Wyoming, debate: a review and critique of models. *The Mountain Geologist* 21, 37–46.
- Stone, D.S., 1993. Basement-involved thrust-generated folds as seismically imaged in the subsurface of the central Rocky Mountain foreland. In: Schmidt, C.J., Chase, R.B., Erslev, E.A. (Eds.), *Laramide Basement Deformation in the Rocky Mountain Foreland of the Western United States*, Special Paper 280. Geological Society of America, pp. 271–318.
- Suppe, J., 1985. *Principles of Structural Geology*. Prentice-Hall, Englewood Cliffs, New Jersey.
- Suppe, J., Medwedeff, D.A., 1984. Fault-propagation folding. *Geological Society of America Abstracts with Programs* 16, 670.
- Walcott, C.D., 1890. Study of line of displacement in the Grand Canyon of the Colorado in northern Arizona. *Geological Society of America Bulletin* 1, 49–64.